




Message in a bottle: First bubble high-speed imagingTuyetthuc Nguyen , Wanjiku Gichigi , and H. C. Mayer **Department of Mechanical Engineering, California Polytechnic State University San Luis Obispo,
San Luis Obispo, California 93407, USA*

(Received 24 May 2023; published 16 November 2023)

This paper is associated with a video winner of a 2022 American Physical Society's Division of Fluid Dynamics (DFD) Milton van Dyke Award for work presented at the DFD Gallery of Fluid Motion. The original video is available online at the Gallery of Fluid Motion, <https://doi.org/10.1103/APS.DFD.2022.GFM.V0036>

DOI: [10.1103/PhysRevFluids.8.110502](https://doi.org/10.1103/PhysRevFluids.8.110502)

When a bottle is filled with liquid, inverted, and emptied, the entry of a slug of air into the neck initiates an incredibly rich and visually compelling sequence of fluid dynamic events. This is especially true for the first bubble to be formed during an emptying process using low-viscosity liquids. Within tenths of a second—fast enough for the unaided eye to miss the details—a slug of air enters the neck, a single bubble is pinched off, and the bubble migrates vertically into the undisturbed liquid within the bottle, all the while evolving as it rises. With further entry of air and outflow of liquid from the bottle, i.e., after the first bubble and when the bottle proceeds with its familiar “glug-glug” [1], the complicated flow field established within the bottle can disturb the evolution of new bubbles and the beauty associated with the first bubble is never recovered.

The motivation for the experiments showcased in the Gallery of Fluid Motion video stemmed from serendipitous still photographs and low-speed movies (i.e., 60 fps) recorded while collecting data on the emptying of bottles [2]. An example is shown in Fig. 1. A subsequent review of the literature revealed limited mention and study of the most interesting feature of the bubble evolution: the liquid jet that forms for bubbles in low-viscosity liquids, i.e., the “microjet” [3] or the “ejector jet” [4]. Hence, the key objectives of the experiments were to use high-speed imaging to photographically capture the first bubble that enters the neck of an inverted bottle and to quantitatively analyze the evolution of that first bubble while paying particular attention to the liquid jet (i.e., measuring the velocity of the jet).

The experimental setup, shown in Fig. 2(a), was designed with simplicity in mind. It utilized a frame of extruded aluminum rail and thin aluminum plates to support an inverted wine bottle which provided nearly unobstructed optical access. A wine bottle of standard size was used [750 mL volume, neck diameter $D_N = 27$ mm, neck length $L_N = 70$ mm, body diameter $D_B = 77$ mm, and total length $L_T = 270$ mm, cf. Fig. 2(b)]. Imaging of the bubble formation and evolution was accomplished using a Phantom v310 high-speed camera recording at either 5 000 fps or 10 000 fps using a frame size of 304×512 pixels. The bottle was backlit using an 18 000-lumen LED panel light and a diffuse screen of sanded acrylic sheet. Seven glycerin-water mixtures, including pure water

*hmayer@calpoly.edu

Published by the American Physical Society under the terms of the [Creative Commons Attribution 4.0 International](https://creativecommons.org/licenses/by/4.0/) license. Further distribution of this work must maintain attribution to the author(s) and the published article's title, journal citation, and DOI.

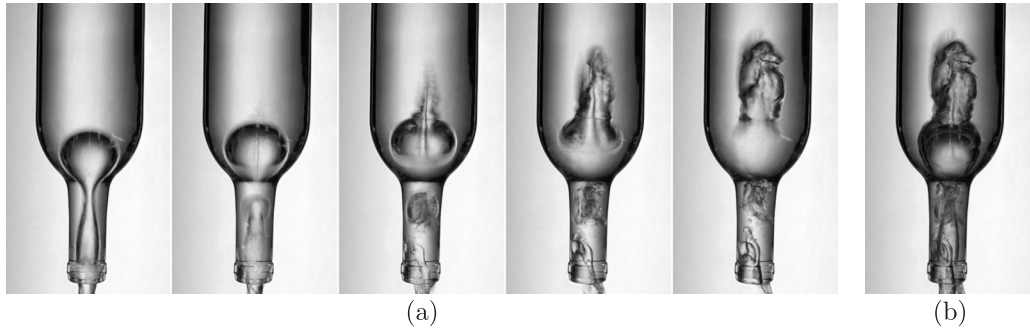


FIG. 1. What do you see? Blurred images extracted from a low-speed movie of bottle emptying using water that motivated further study (Nikon D3400, 60 fps, ~ 16 ms exp). (a) Five sequential frames with blurred features spanning 70 ms. (b) Overlay of five frames is similar to what our eye sees, i.e., the details are hidden.

and pure glycerin, were used and provided a wide range of liquid viscosity of $\mu = 1\text{--}1410$ cp, along with relatively small changes in density and air-liquid surface tension, i.e., $\rho_l = 1.00\text{--}1.26$ g/cm³ and $\sigma = 72\text{--}63$ mN/m, respectively. A sequence of images, captured using the experimental setup described and showing key stages in the evolution and breakup of the first bubble, is provided in Fig. 3. Note the dramatic contrast with the blurry images in Fig. 1 as details emerge with higher frame rates and shorter exposure times (10 000 fps and 0.01 ms exp versus 60 fps and 16 ms exp).

Quantitative information about the first bubbles, e.g., size and jet velocity, was acquired using a MATLAB image processing program developed by a team of undergraduate students. The low resolution of the high-speed movies required that key features be manually identified in the frames chosen for analysis. By selecting several points along the air-liquid interface, bubble size information could be estimated through a fit of an ellipse, and by tracking the tip of the liquid jet formed by the retracting tail of the bubble after pinch-off, the velocity of the jet tip could be calculated. Representative images and data collected from an experiment with water are shown in Fig. 4. The images in Fig. 4(a) show how the MATLAB image processing program measures the size, and tracks the center, of the bubble along with the jet tip. An ellipse [blue line in (i)–(iv)] is fit to four points manually selected on the surface of the bubble in each frame chosen for analysis, and this is used to estimate the volume and equivalent diameter of the bubble. The center of the ellipse (red circle) is automatically located. The location of the jet is manually identified as it evolves (blue dot and white arrow), i.e., starting with bubble pinch-off (i), through jet formation (ii), impact (iii), and penetration (iv). Referring to the blue ellipses in (i)–(iv), we can see that during these stages the size

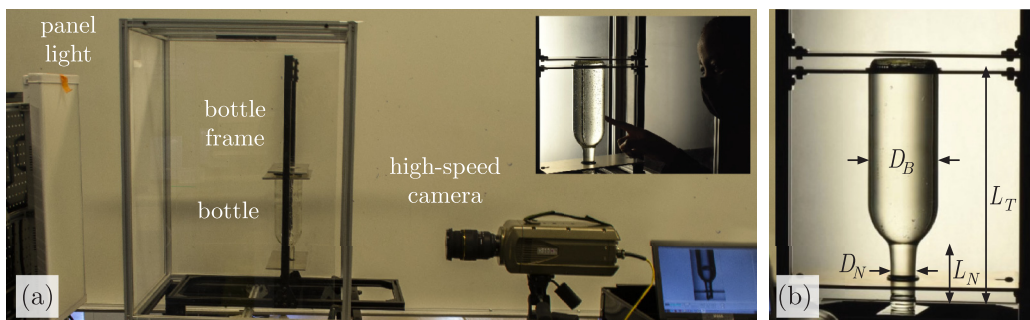


FIG. 2. Experimental setup for collecting high-speed movies of the first bubble. (a) Main components of the setup include a high-speed camera, bottle, frame, and panel light. (b) Relevant bottle dimensions (bottle illuminated from behind by panel light in this image).

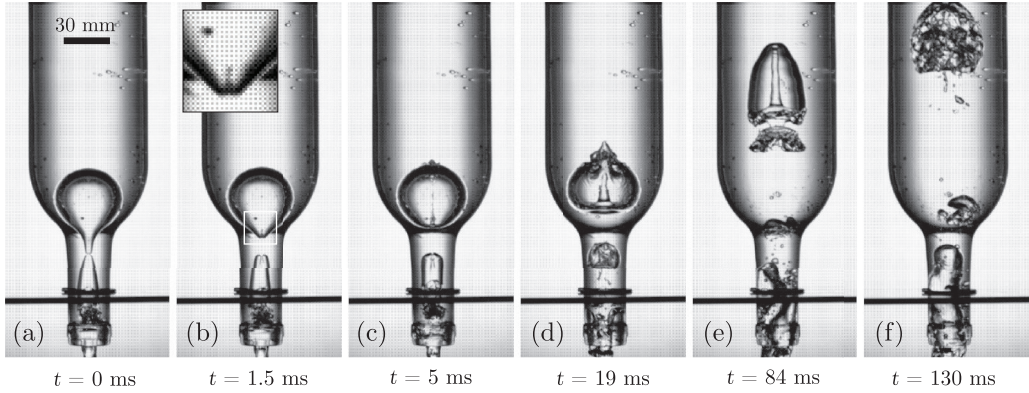


FIG. 3. The key stages of the formation, evolution, and breakup of the first bubble. For this case the liquid is water (same bottle and liquid as Fig. 1). (a) Pinch-off of bubble from a slug of air in the neck. (b) As the tail of the bubble retracts, it leads to the formation of a small-scale liquid jet (i.e., the “ejector jet” [4]). (c) The tip of the jet travels across the bubble and impacts the top. (d) Complete penetration of the bubble by the jet occurs a short time later. (e) The jet continues to travel upward and creates an annular bubble structure with a liquid core. (f) The vertical motion of the liquid core continues as the bubble disintegrates. Liquid viscosity will dictate which key stages are observed.

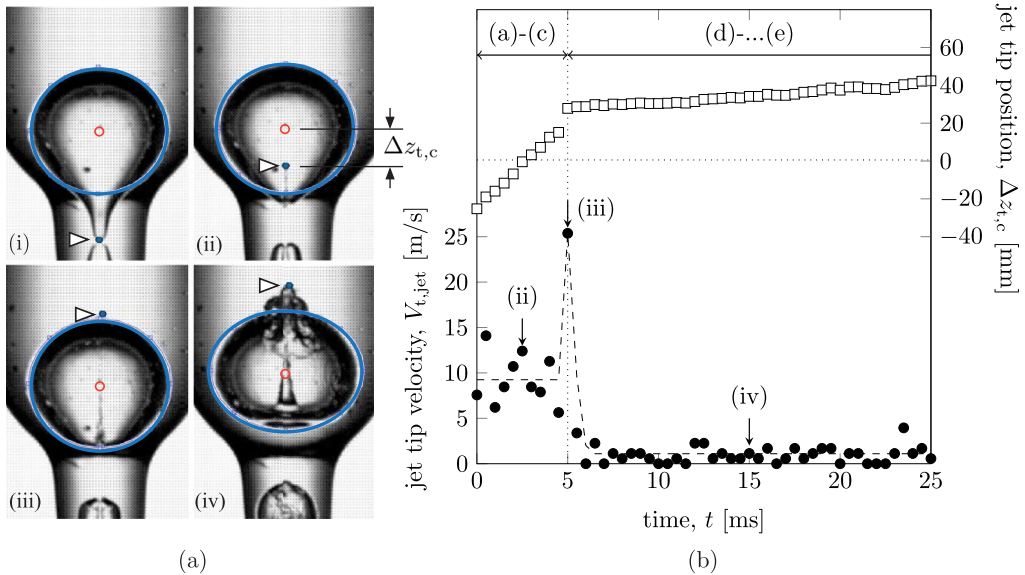


FIG. 4. Representative images and data plot illustrating MATLAB image processing results from high-speed movie analysis using water. Using manual identification on a frame-by-frame basis, the jet tip position and velocity, and the approximate bubble shape and size, can be tracked over time. (a) Images show the location of the jet tip (white arrow), the approximate outline of the bubble (blue ellipse), and the center of bubble (red circle). The location of the jet tip position with respect to the center of the bubble $\Delta z_{t,c}$ takes on negative values at pinch-off and jet formation (i and ii), and becomes positive as the jet impacts and penetrates the top of the bubble (iii and iv). (b) A plot of jet tip velocity $V_{t,jet}$ shows an order of magnitude of ~ 10 m/s, with a lower ~ 1 m/s magnitude as the jet continues to penetrate the bubble.

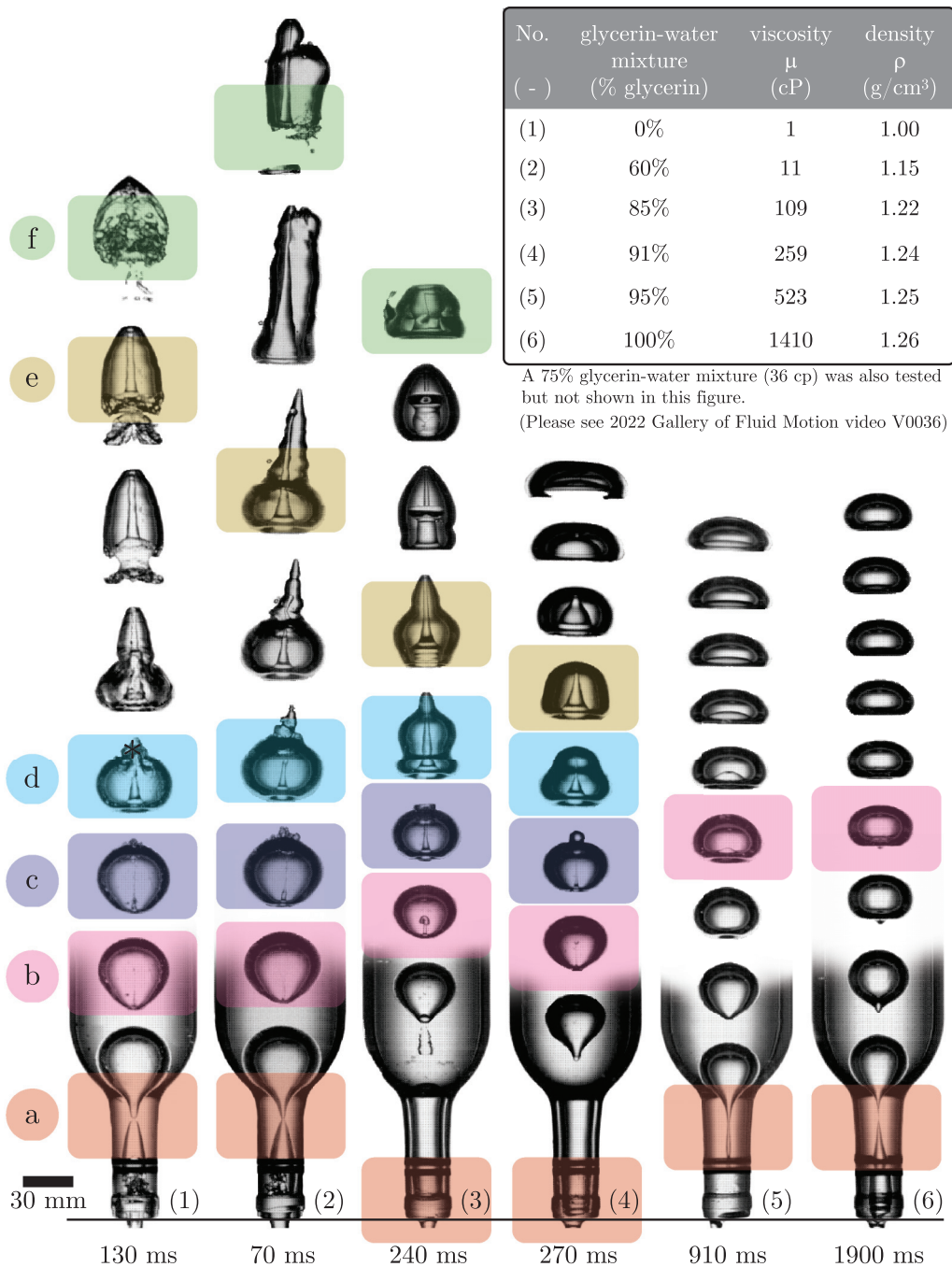


FIG. 5. Montage of bubble formation, evolution, and breakup for six different liquids (1)–(6). Labels (a)–(f), color coded across images, correspond directly to the stages (a)–(f) outlined and discussed in Fig. 3. The time listed beneath each sequence indicates the total time elapsed from pinch-off (bottom of figure) to the final frame of each high-speed movie where the bubble has reached the top of the field of view. Note that as viscosity increases, left to right in the figure, the evolution of the bubble changes dramatically. With increasing liquid viscosity, the liquid jet no longer penetrates the bubble, annular bubble shapes no longer form, and the type of disintegration seen at lower viscosity is replaced with a steady shape.

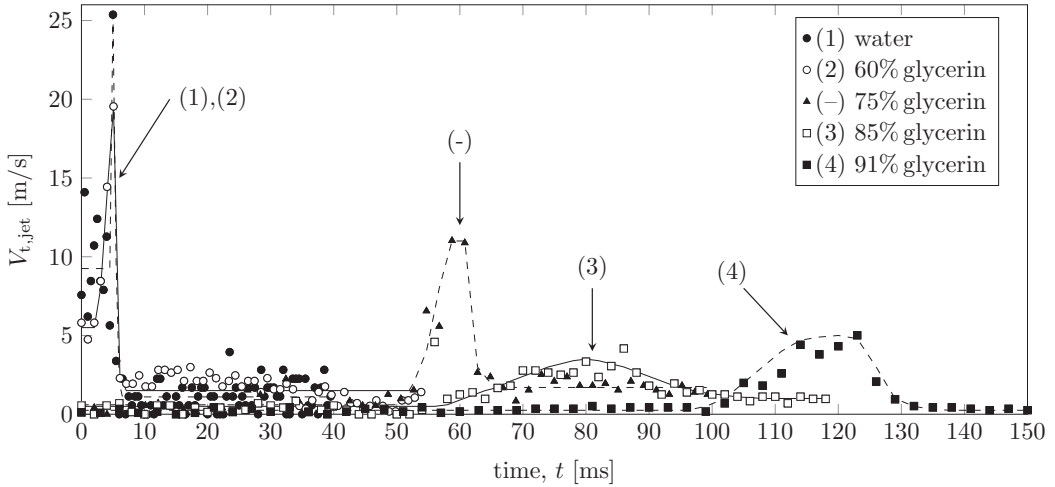


FIG. 6. Measurements of jet tip velocity show a decrease in velocity and delay in maximum velocity with increasing liquid viscosity. Liquid viscosity numbers correspond to inset in Fig. 5. Lines through data have been included to guide the eye. Scatter of measurements for any liquid is related to manual nature of feature identification in image processing and low resolution of movie images.

and shape of the bubble remains somewhat unchanged, but after complete penetration of the jet, the bubble can take on much different shapes [e.g., Figs. 3(e) and 3(f)]. Frame rate and feature location information can be used to quantitatively characterize the jet tip as shown in Fig. 4(b). Not shown in this figure is information about the bubble rise velocity U , which tends to be much less than the jet tip velocity $V_{t,jet}$, i.e., $U \sim 0.1\text{--}0.5$ m/s as compared to $V_{t,jet} \sim 1\text{--}10$ m/s. From the range of glycerin-water mixtures tested, bubble sizes were found to be in the range of approximately $D \sim 36\text{--}48$ mm, with bubble size generally decreasing as liquid viscosity increases.

For the case of individual bubbles rising steadily in undisturbed liquids, the shape regime of the bubble is set by the Eötvös number [$Eo = g(\rho_l - \rho_g)D^2\sigma^{-1}$], Morton number [$M = g\mu^4(\rho_l - \rho_g)\rho_l^{-2}\sigma^{-3}$], and Reynolds number ($Re = \rho_l DU\mu^{-1}$) [5]. Within these equations, g is gravity, ρ is fluid density (with g and l subscripts denoting gas and liquid phases, respectively), μ is liquid viscosity, D is bubble diameter, U is bubble rise velocity, and σ is the gas-liquid surface tension. The Eötvös number can be considered a ratio of body to surface forces, the Reynolds number a ratio of inertia to viscous forces, and the Morton number a dimensionless group composed only of fluid properties (i.e., it is defined that there is no length scale or characteristic velocity) relevant to establishing the shape of bubbles. In the experiments presented here, $\rho_l \gg \rho_g$, and since D , ρ_l , and σ do not change substantially for our liquids, neither does Eo , which has values of ~ 300 for all liquids tested. In addition, changes in M are driven mainly by changes in μ , as is the case for Re . Thus, for experiments involving a fixed bottle shape (helping to set the first bubble size), changes in glycerin-water mixture can be thought of in terms of changing Re and M , which take on ranges of $\sim 10\text{--}18\,000$ and $\sim 10^2\text{--}10^{-11}$, respectively.

If the height of the bottle allowed for all first bubbles to reach a steady condition, we would expect from our range of Re and M that the bubbles would take on spherical-cap shapes for low-viscosity liquids (high Re and low M), skirted shapes for intermediate Re and M , and dimpled ellipsoidal-cap shapes for high-viscosity liquids (low Re and low M) as glycerin quantity is increased [5]. However, the evolution of the first bubble from an inverted bottle can often produce no steady shape for lower-viscosity liquids (e.g., 0–85% glycerin content). This is because the limited height of the bottle, coupled with the larger bubble rise speeds and the more complicated shape evolution after complete jet penetration, provides an insufficient distance and time for a steady bubble shape to be

realized. Although captured better in the Gallery of Fluid Motion video, Fig. 5 shows the myriad behavior and beauty in the first bubble formation and evolution as μ increases (left to right). In particular, low-viscosity liquids develop the ejector jet, which can completely penetrate the rising bubble, causing it to break up in dramatic fashion, whereas high-viscosity liquids begin to take on steady predictable shapes toward the top of the bottle.

Perhaps the most interesting feature associated with the first bubble formed in low-viscosity liquids is the ejector jet which dominates the evolution of the bubble. As seen for the case of water in Fig. 4, the jet tip velocity can reach values of ~ 10 m/s during the first few milliseconds after pinch-off. As shown in Fig. 5, the nature of the ejector jet and its influence are changed with liquid viscosity. In particular, for lower-viscosity liquids [e.g., Fig. 5 liquids (1)–(3)], the speed of the ejector jet allows it to fully penetrate the bubble, leading to annular bubble shapes prior to breakup. As liquid viscosity increases, ejector jet speed decreases and the jet can hardly penetrate or no longer penetrate the bubble in a similar fashion [cf. Fig. 5 liquid (4)]. Finally, for the highest-viscosity liquids [e.g., Fig. 5 liquids (5) and (6)], the tail of the bubbles simply retract at low speed after pinch-off, creating a small dimple at the trailing edge. These qualitative descriptions are supported by quantitative measurements of jet tip velocity for different glycerin-water mixtures. Figure 6, in dimensional form for ease of interpretation, demonstrates that as liquid viscosity increases, the magnitude of the jet tip velocity decreases. Furthermore, the time after pinch-off associated with the maximum jet tip velocity increases, consistent with a slower retraction and formation of the ejector jet.

This work was supported by the Cal Poly SLO Office of University Diversity and Inclusion's (OUDI) BEACoN Research Mentoring Program in addition to the Cal Poly SLO ME Department Constant J. and Dorothy F. Chrones Endowed Professorship.

-
- [1] C. Clanet and G. Searby, On the glug-glug of ideal bottles, *J. Fluid Mech.* **510**, 145 (2004).
 - [2] H. C. Mayer, Bottle emptying: A fluid mechanics and measurements exercise for engineering undergraduate students, *Fluids* **4**, 183 (2019).
 - [3] K. Kondo, K. Yoshida, T. Matsumoto, T. Okawa, and I. Kataoka, Flow patterns of gas-liquid two-phase flow in round tube with sudden expansion, *Proceedings of ICONE10*, 22154 (2002).
 - [4] L. Rohilla and A. K. Das, Fluidics in an emptying bottle during breaking and making of interacting interfaces, *Phys. Fluids* **32**, 042102 (2020).
 - [5] R. Clift, J. R. Grace, and M. E. Weber, *Bubbles, Drops, and Particles* (Dover Publications, New York, 2013).